Shoaling of subharmonic gravity waves

J. A. Battjes,[1] H. J. Bakkenes,[1,2] T. T. Janssen,[1] and A. R. van Dongeren[3]

Received 20 March 2003; revised 31 October 2003; accepted 14 November 2003; published 13 February 2004.

[1] In this paper the energy budget of wave group-induced subharmonic gravity waves in the nearshore region is examined on the basis of the energy equation for long waves in conjunction with analyses of a high-resolution laboratory data set of one-dimensional random wave propagation over a barred beach. The emphasis is on the growth of forced subharmonics and the deshoaling of the reflected free waves in the shoaling zone. The incident lower-frequency subharmonics are nearly fully reflected at the shoreline, but the higher-frequency components appear to be subject to a significant dissipation in a narrow inshore zone including the swash zone. The previously reported phase lag of the incident forced waves behind the short-wave groups is confirmed, and its key role in the transfer of energy between the grouped short waves and the shoaling bound waves is highlighted. The cross-shore variation of the local mean rate of this energy transfer is determined. Using this as a source function in the wave energy balance allows a very accurate prediction of the enhancement of the forced waves in the shoaling zone, where dissipation is insignificant. The phase lag appears to increase with increasing frequency, which is reflected in a frequency-dependent growth rate, varying very nearly from the free-wave variation $\sim h^{-1/4}$ (Green's law) for the lower frequencies to the shallow-water equilibrium limit for forced subharmonics $\sim h^{-5/2}$ for the higher frequencies. This observed frequency dependence is tentatively generalized to a dependence on a normalized bed slope, controlling whether a so-called mild-slope regime or a steep-slope regime prevails, in which enhanced incident forced waves dominate over breakpoint-generated waves or vice versa. *INDEX TERMS:* 4546 Oceanography: Physical: Nearshore processes; 4560 Oceanography: Physical: Surface waves and tides (1255); *KEYWORDS:* surface waves, infragravity waves, surfbeat, bound waves, wave shoaling, energy transfer

Citation: Battjes, J. A., H. J. Bakkenes, T. T. Janssen, and A. R. van Dongeren (2004), Shoaling of subharmonic gravity waves, *J. Geophys. Res.*, *109*, C02009, doi:10.1029/2003JC001863.

1. Introduction

[2] The pioneering observations by *Munk* [1949] and *Tucker* [1950] first brought to light the existence of low-frequency (lf) waves in the coastal zone, correlated to incident groups of high-frequency (hf) waves (wind waves and/or swell). Because these lf waves were believed to have been generated in the surf zone as a result of a beat (subharmonic) phenomenon induced by the narrow-band incident wind-generated waves, they were called surf beat. (These subharmonic motions are also referred to as infragravity waves; we do not want to use this term since it refers to a frequency band below that of the gravity waves, which is not appropriate here.) Because of their theoretical and practical importance, they have been studied extensively, theoretically as well as through laboratory experiments and field observations. For detailed reviews, reference is made to recent papers on the subject [*Baldock et al.*, 2000; *Baldock and Huntley*, 2002; *Sheremet et al.*, 2002; *Reniers et al.*, 2002; *Janssen et al.*, 2003]. The following comments as well as the remainder of this paper are restricted to one-dimensional (cross-shore) propagation.

[3] Two main mechanisms of generation of cross-shore lf wave motions by grouped sea/swell waves have been recognized. One is the quadratic difference interaction among pairs of primary waves, resulting in group-bound long second-order waves [*Biésel*, 1952; *Longuet-Higgins and Stewart*, 1962]. These accompany incident sea/swell waves from deep water, and are subsequently enhanced over the sloping seabed in the nearshore zone as a result of the continual forcing by the shoaling primary waves, up to the zone of initial breaking [e.g., *List*, 1992; *Masselink*, 1995], or even within the surf zone [*Foda and Mei*, 1981; *Schäffer and Svendsen*, 1988]. The other mechanism is the generation of free waves by a moving breakpoint [*Symonds et al.*, 1982; *Symonds and Bowen*, 1984]. *Schäffer and Jonsson* [1990] and *Schäffer* [1993] gave a formulation for the combination of both mechanisms.

[4] Laboratory observations on a steep beach (slope 1:10) by *Baldock et al.* [2000] and *Baldock and Huntley* [2002] have indicated a clear dominance of breakpoint-generated waves. However, no published field observations known to

[1]Section of Environmental Fluid Mechanics, Faculty of Civil Engineering and Geosciences, Delft University of Technology, Delft, Netherlands.
[2]Now at Heerema Marine Contractors, Leiden, Netherlands.
[3]WL/Delft Hydraulics, Delft, Netherlands.

0148-0227/04/2003JC001863

the authors have given indications of an observable contribution from breakpoint-generated free waves to the total wave-induced lf energy in the nearshore zone. It is likely that this is due to the fact that the bed slopes in the published field cases, of the order of a few percent, were much less than in the laboratory experiments referred to. The same is true for the laboratory experiments by *Boers* [1996], where the bed slope in the shoaling zone was about 1:70. Analyses of the latter data by *Janssen et al.* [2003] gave no indication of generation by a moving breakpoint. *List* [1992] and *van Dongeren et al.* [2002] have indicated that the importance of breakpoint generation relative to (enhancement of) incident bound waves increases with increasing bed slope. We return to this question below.

[5] Numerical studies as well as observations indicate that the rate of growth of shoaling bound waves as a function of the local depth is higher than for free long waves (Green's law), but less than it would be if the equilibrium theory of *Longuet-Higgins and Stewart* [1962] were applied over a sloping bed. Despite the abundance of numerical models, systematic dependencies controlling the actual growth rate have not yet been established, even in the most reduced case of one-dimensional propagation in absence of dissipation. The present paper attempts to shed some light on these questions, restricted to shore normal motions. Results of a set of laboratory data with high spatial resolution [*Boers*, 1996] are utilized for a detailed analysis. We determine, among others, the local, frequency-resolved rate of energy transfer from the primary waves to the shoaling forced waves, instead of merely the cross-shore variation of the total forced wave energy, so as to gain more insight in the underlying processes.

2. Existing Model Formulations

[6] In this section we review theoretical models that are relevant in the context of shoaling forced subharmonic waves.

2.1. Uniform Depth: Equilibrium Solution

[7] The existence of group-bound subharmonic waves appears to have been first pointed out by *Biésel* [1952], who presented the second-order (in wave steepness) Stokes-type solution for a long-crested wave system in uniform depth, which to first order consists of an arbitrary number of sinusoidal component waves of arbitrary frequency and (small) amplitude, traveling in the same direction (purely progressive system) or partly or wholly in opposite directions (including partial or complete standing wave system). The solution contains bound superharmonics and subharmonics of pairs of interacting primary components. As a special case, Biésel presented the equations for a narrow-banded set of progressive primary waves, and noted that the difference interactions therein give rise to group-bound long waves in antiphase with the envelope of the primary waves.

[8] Apparently unaware of Biésel's work, *Longuet-Higgins and Stewart* [1962] (hereinafter referred to as LHS62) presented the result to second order in wave steepness of the difference interactions among pairs of a set of primary waves of closely neighboring frequencies, again for one-dimensional (1-D) propagation. *Hasselmann* [1962] derived more general expressions correct to second order including all sum and difference interactions between pairs of components for the two-dimensional (2-D) case, not restricted to narrowbandedness. The theoretical results by LHS62 (1-D) and Hasselmann (2-D) for the forced long waves have since become widely used and have been validated against observational data in the laboratory (1-D) [e.g., *Kostense*, 1984; *Baldock et al.*, 2000] and in the field (2-D) [e.g., *Herbers et al.*, 1994].

[9] Assuming a steady state equilibrium solution for the case in which the short-wave groups are much longer than the water depth, LHS62 expressed the surface elevation of the accompanying forced waves (ζ) in terms of the radiation stress delivered by the primary waves (S_{xx}) according to

$$\zeta(x,t) = -\frac{S_{xx}(x,t)}{\rho\left(gh - c_g^2\right)} + \text{const} \tag{1}$$

in which ρ is the fluid density, g the gravitational acceleration, h the mean depth, c_g the group velocity of the narrow-banded primary wave system and x a horizontal coordinate in the direction of wave propagation. The response given by equation (1) approaches resonance if the primary waves are effectively in shallow water ($kh \ll 1$). In that case, $c_g^2 = gh[1 - (kh)^2 + O(kh)^4]$ and (omitting the constant) equation (1) can to order $(kh)^2$ be approximated as

$$\zeta \cong -\frac{S_{xx}}{\rho g h (kh)^2} \cong -\frac{S_{xx}}{\rho \sigma^2 h^2} \tag{2}$$

in which k and σ are the characteristic wave number and frequency of the primary wave system (LHS62). Thus other things (including S_{xx}) being equal, the shallow-water low-frequency response varies with depth (assumed spatially uniform) as h^{-2}.

2.2. Sloping Bottom: Quasi-Uniform Depth Approximation

[10] It is important to note that the results summarized above represent bound waves of constant form propagating over a horizontal bottom. They cannot be applied to shoaling waves over a sloping bottom without further justification. We return to this below. If, for the time being, this approach is accepted, the variation of S_{xx} must be specified. Assuming conservation of short-wave energy, the value of S_{xx} increases with decreasing depth, whereas the denominator in equation (1) decreases, so that the response increases. In very shallow water, such that $kh \ll 1$, equation (2) applies and (still assuming conservation of short-wave energy), $S_{xx} \sim h^{-1/2}$, so that the bound-wave amplitude would vary $\sim h^{-5/2}$ as $kh \to 0$ (LHS62).

[11] It should be pointed out that LHS62 correctly make the necessary reservations with respect to the applicability of the steady wave results to shoaling waves, by noting that the solution cannot depend on the local depth only, but must depend on the entire form of the bottom profile because of the expected appreciable depth variation within a distance equal to the length of a wave group. Referring to the applicability of the near-resonant solution (2) over a sloping bottom, they state that its validity is limited (among others) by the fact that the resonance needs time to build up. On the

other hand, *Longuet-Higgins and Stewart* [1964] also indicate that if the bottom slope is sufficiently gentle, so that dynamical equilibrium has time to be established, $\zeta \sim h^{-5/2}$. The conditions for which this applies have not yet been established and are investigated below.

[12] Several authors implicitly or explicitly consider the horizontal bottom equilibrium solution as a theoretical shoaling law for bound waves over a sloping bottom. For example, the deviation of the observed cross-shore amplitude variation from a $h^{-5/2}$ dependence has been used to support conclusions about the presence or relative importance of forced long waves in a wave field [*Elgar et al.*, 1992; *Ruessink*, 1998a, 1998b]. However, the equilibrium solution cannot a priori, without the necessary constraints, be considered applicable to waves over a sloping bottom.

2.3. Mild Slope Approximations

[13] A wide variety of models for the calculation of bound waves over a shoaling bottom has been developed. The effects of a stepwise varying bathymetry on the subharmonic response has been studied by *Molin* [1982] for normal wave incidence and deep water conditions for the primary (forcing) waves. This was extended for sloping bottoms by *Mei and Benmoussa* [1984], assuming oblique incident waves and intermediate water depth for the forcing waves, on the basis of a WKB-type expansion previously described by *Chu and Mei* [1970]. Part of this is reexamined by *Liu* [1989]. *Liu and Dingemans* [1989] have extended the formulation to arbitrary, mildly sloping bathymetry in two dimensions including bottom-induced scattering. Deterministic and stochastic frequency domain evolution models for shoaling primary waves, accounting for quadratic wave-wave interactions have also been developed, on the basis of the classical long-wave equations [e.g., *Van Leeuwen and Battjes*, 1990; *Van Leeuwen*, 1992; *Janssen et al.*, 2003], Boussinesq equations [e.g., *Freilich and Guza*, 1984; *Madsen and Sørensen*, 1993; *Herbers and Burton*, 1997] and fully dispersive second-order theory [e.g., *Kaihatu and Kirby*, 1995; *Agnon and Sheremet*, 1997; *Eldeberky and Madsen*, 1999]. Last, we mention direct numerical integration of (short-wave resolving) Boussinesq equations [*Madsen et al.*, 1997] or of the (short-wave-averaged) radiation stress forced shallow-water equations [e.g., *List*, 1992; *Roelvink et al.*, 1992; *Roelvink*, 1993; *van Dongeren*, 1997; *Reniers et al.*, 2002; *van Dongeren et al.*, 2003].

[14] All of these models require numerical integration to establish the local solution at an arbitrary location, because it depends on the entire bottom profile, as pointed out by LHS62. Overall, comparisons with observations have confirmed the predictive capability of these numerical models, but general trends in amplitude variation have not been established.

3. Energy Transfer to Shoaling Forced Waves

[15] Application of the equilibrium relationship given by equation (1) over a sloping seabed yields a growth rate of the forced waves exceeding the rate for free long waves (Green's law), implying an energy transfer to these waves as they shoal. Adopting the concept and formulation by *Longuet-Higgins and Stewart* [1961, equation [9.2]] this energy is delivered by the primary waves through gradients in the radiation stress.

[16] In the steady state, and in absence of dissipation, the energy balance for forced low-amplitude progressive long waves can be written as [*Phillips*, 1977]

$$\frac{\mathrm{d}F}{\mathrm{d}x} = R \equiv -\left\langle U \frac{\mathrm{d}S_{xx}}{\mathrm{d}x} \right\rangle \tag{3}$$

in which F is the phase-averaged energy flux per unit span by the forced waves, R is the phase-averaged rate of work per unit area done on the forced waves by the short-wave radiation stress S_{xx}, U is the depth-averaged long-wave particle velocity, and the angular brackets denote phase averaging.

[17] In the constant depth equilibrium situation, there should be no net energy transfer between primary waves and bound waves, which is in agreement with the phase difference π between the bound wave and the radiation stress, expressed in equation (1) (so that the stress gradient and the bound wave particle velocity are in quadrature, resulting in a zero cycle-averaged energy transfer). For a net time-averaged transfer to be possible, there must be an additional phase shift, say $\Delta\psi$ (here defined as the phase lag of a bound wave minimum elevation behind a maximum of the envelope of the primary waves). This implies that local application of the equilibrium solution for the amplitude on a sloping bottom is in a sense inconsistent: the amplitude variation implies energy supply and therefore a phase lag different than the equilibrium value of π.

[18] Numerous authors have observed that shoaling bound waves are lagging (increasingly) in phase behind the primary wave groups (the equilibrium phase lag of π will be understood from here on), in the field [*Elgar and Guza*, 1985; *List*, 1992; *Masselink*, 1995] as well as in the laboratory [*Mansard and Barthel*, 1984; *Janssen et al.*, 2000, 2003]. Similar lags have resulted from numerical calculations in the time domain [*List*, 1992; *Madsen et al.*, 1997; *van Dongeren*, 1997] and in the frequency domain [*Herbers and Burton*, 1997]. The existence of such phase lag has been shown analytically by *Bowers* [1992], *Van Leeuwen* [1992] and *Janssen et al.* [2003].

[19] The dynamical significance of this phase lag is that it implies the possibility of a net energy transfer to the forced waves, as required for observed growth rates exceeding Green's law. This fact has been pointed out and exploited by *van Dongeren* [1997] and *van Dongeren et al.* [2002]. Other than this, it does not seem to have received much attention. We will investigate this process in detail, on the basis of a laboratory data set obtained by *Boers* [1996], characterized by a high spatial resolution, allowing a frequency-resolved evaluation of local energy densities and fluxes considered separately for ingoing and outgoing waves. Following the description and analysis of these data, we return to the question which parameter(s) control(s) the enhancement of the shoaling forced waves and whether generalizable growth rates can be established.

4. Experimental Data

[20] *Boers* [1996] carried out experiments in a wave flume (L × W × H = 40 m × 0.80 m × 1.05 m) of the

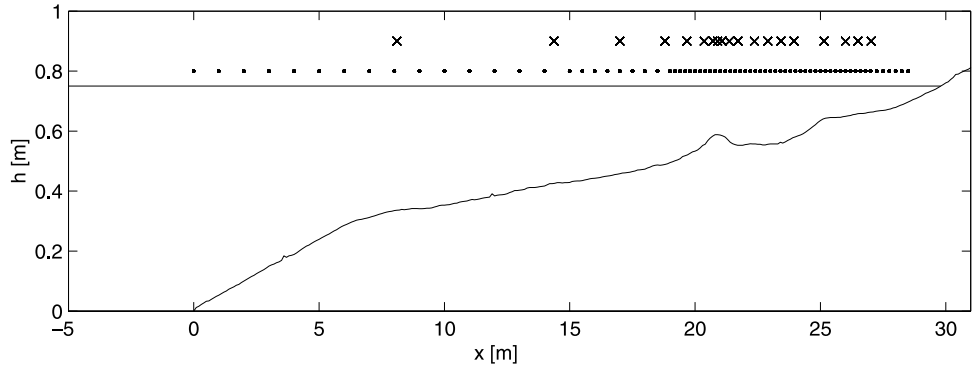

Figure 1. Cross-shore bottom profile and still water level in Boers' experiments. Dots and crosses represent cross-shore locations of surface elevation gauges and velocity sensors, respectively.

Fluid Mechanics Laboratory of Delft University of Technology. The flume was equipped with a hydraulically driven piston type wave generator with second-order control [*Van Leeuwen and Klopman*, 1996], suppressing generation of free superharmonics and subharmonics. Active Reflection Compensation was used to minimize rereflections at the wave board. Wave control signals with a duration of 245.4 s were generated and repeated 7–11 times per run, so that wave conditions were irregular but deterministic and reproducible. The fixed, smoothed concrete bottom profile used in the experiments, a mimic of a sandy beach profile, is shown in Figure 1. A horizontal bottom part of 5 m long extends between the wave generator (midpoint of the wave board position at $x = -5$ m) to the toe (at $x = 0$ m) of a short, relatively steep (≅1:20) approach slope leading to a longer, more gentle (≅1:70) slope and two bars. Using repeated runs with the same control signals, synchronized surface elevation measurements were conducted at 70 cross-shore locations (indicated by dots in Figure 1). Velocity measurements were conducted at 17 different cross-shore locations (indicated by crosses in Figure 1) over a number of points in the vertical. The measurement sampling frequency was 20 Hz.

[21] Experiments were carried out with a still water depth of 0.75 m in the constant depth section for three different wave conditions. In this paper only the low-steepness wave condition (1C), in which the shoaling of hf and lf waves is most evident, will be analyzed, with peak frequency f_p = 0.29 Hz and initial significant wave height $H_{m_0,hf} = 0.10$ m (defined as four times the standard deviation of the hf surface elevation for frequencies between 0.20 Hz and 1 Hz). For this condition, there was virtually no breaking offshore of the outer bar near $x = 21$ m (Boers, personal communication). This is borne out by the cross-shore variation of the hf significant wave height $H_{m_0,hf}$, shown in Figure 2. The shoaling up to the outer bar is clearly visible as well as the locally enhanced decay over the outer bar and the inner bar.

[22] The high spatial resolution of the surface elevation measurements makes it possible to use a quasi-continuous presentation of the variance density in space, as shown in

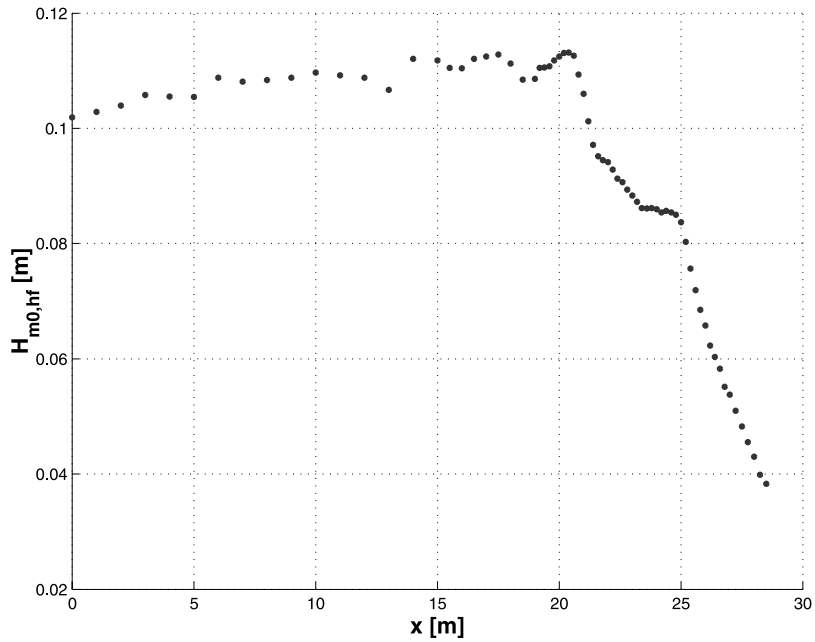

Figure 2. Cross-shore variation of hf significant wave height.

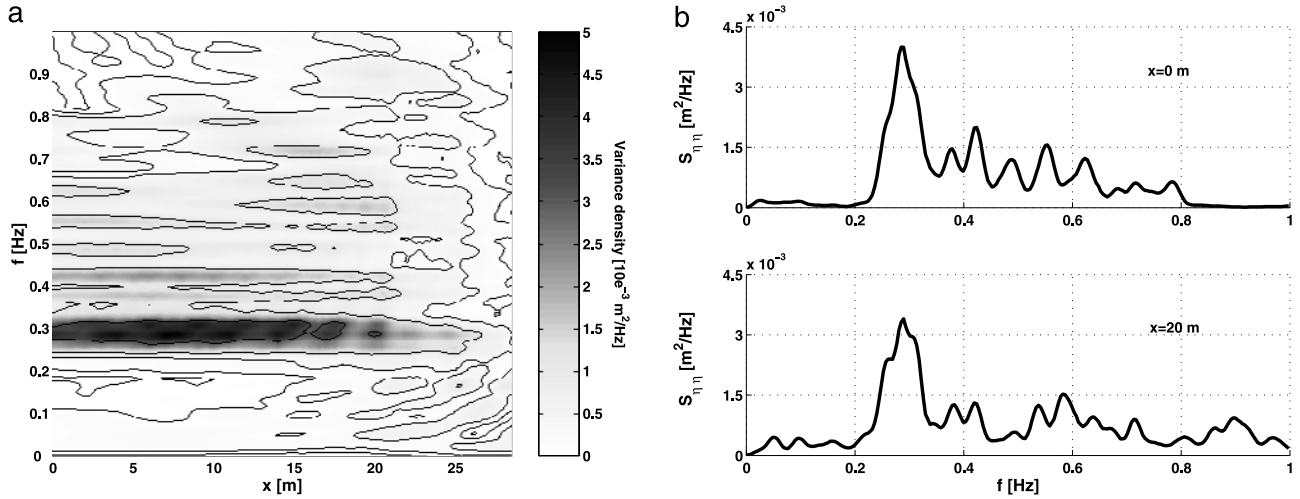

Figure 3. (left) Spatial evolution of the variance density spectrum of the measured surface elevation; density ratio for adjacent iso-density curves is $10^{0.5}$. (right) Surface elevation variance density spectra at two cross-shore locations.

Figure 3 (left). The values shown were obtained by frequency averaging of raw estimates with a Hamming window of 12 points, giving 13 DOF and a resolution of 0.026 Hz. The dark bar represents the region of maximum variance densities near the incident peak frequency f_p = 0.29 Hz. It shows weak rhythmic cross-shore variations that may be shown to fit a nodal structure corresponding to (partial) reflection at the waterline for $f = f_p$, thus signaling a weak reflection of the hf energy, which however is ignored in the following. Shoreward from the outer bar (crest near $x = 21$ m), a strong decrease of the variance density of the hf waves is observed, because of wave breaking. At $x = 28$ m most of the incident hf wave energy was lost (about 95%) [*Boers*, 1996]. Figure 3 (right) shows the spectra of surface elevation at two cross-shore locations, one offshore and the other near the outer bar.

[23] Curved spectral ridges and troughs are visible in the low-frequency, nearshore region in Figure 3 (left). These correspond to a nodal structure of the lf waves, indicating that the lf wave field is a superposition of shoreward and seaward propagating components. *Janssen et al.* [2003] present a detailed analysis of the lf wave signals. Using cross correlations with high spatial resolution, the incoming lf waves were shown to propagate shoreward at a speed slightly less than the group velocity of the primary wave (the peak frequency value). The outgoing wave speed matches very closely the free long-wave speed. This is utilized below for the separation of the total signal in an incoming and an outgoing component.

5. Amplitude Variation of Incoming and Outgoing lf Waves

[24] Because we are primarily interested in the process of energy transfer to the forced waves, we separate the signal of the total lf motion in incoming and outgoing components using an array method, based on surface elevation data at a number of adjacent wave gauges. We use a least squares estimation procedure [*Zelt and Skjelbreia*, 1992], modified for a nonuniform water depth [see also *Baldock and Simmonds*, 1999]. As a check, we make point estimates based on colocated data on surface elevation and horizontal particle velocity [*Guza et al.*, 1984] at the (fewer) locations where these are available.

[25] In view of the applied second-order wave board control, which suppresses generation of free harmonics, and active reflection compensation at the wave board, we assume in the analyses to follow that the incoming lf signal is due to bound subharmonics only.

5.1. Separation Procedure

[26] In so-called array methods the incoming and outgoing lf waves at a certain location are estimated using surface elevation measurements at a number of adjacent wave gauges, a so-called local array. The decomposition is carried out in the frequency domain, on the basis of surface elevations for a local wave gauge array consisting of P gauges ($p = 1,\ldots P$) in locations x_p centered around a reference location x_r. The complex amplitude of the mth harmonic of the total signal at x_p is denoted by $Z_{m,p}$:

$$Z_{m,p} = \frac{1}{N}\sum_{j=1}^{N} \zeta(x_p, t_j) e^{-i2\pi f_m t_j} \tag{4}$$

where j is a time counter, N is the total number of data points per time series and $f_m = m/D$, with $m = 0, \pm1, \pm2,..$ (two sided) and D the record duration. $Z_{m,p}$ is taken to be the sum of an incoming ($Z^+_{m,p}$) and an outgoing component ($Z^-_{m,p}$). The values of these at the reference location x_r are estimated from the set of equations given by

$$Q^+_{m,p,r} Z^+_{m,r} + Q^-_{m,p,r} Z^-_{m,r} = Z_{m,p} \; for \; p = 1,\ldots,P \tag{5}$$

The operators $Q^+_{m,p,r}$ and $Q^-_{m,p,r}$ account for amplitude and phase variation of the mth harmonic between reference location x_r and location x_p for the incoming and outgoing waves respectively, assuming linear propagation and conservation of energy. Even though this is not necessarily correct for the forced waves, it is expected to give

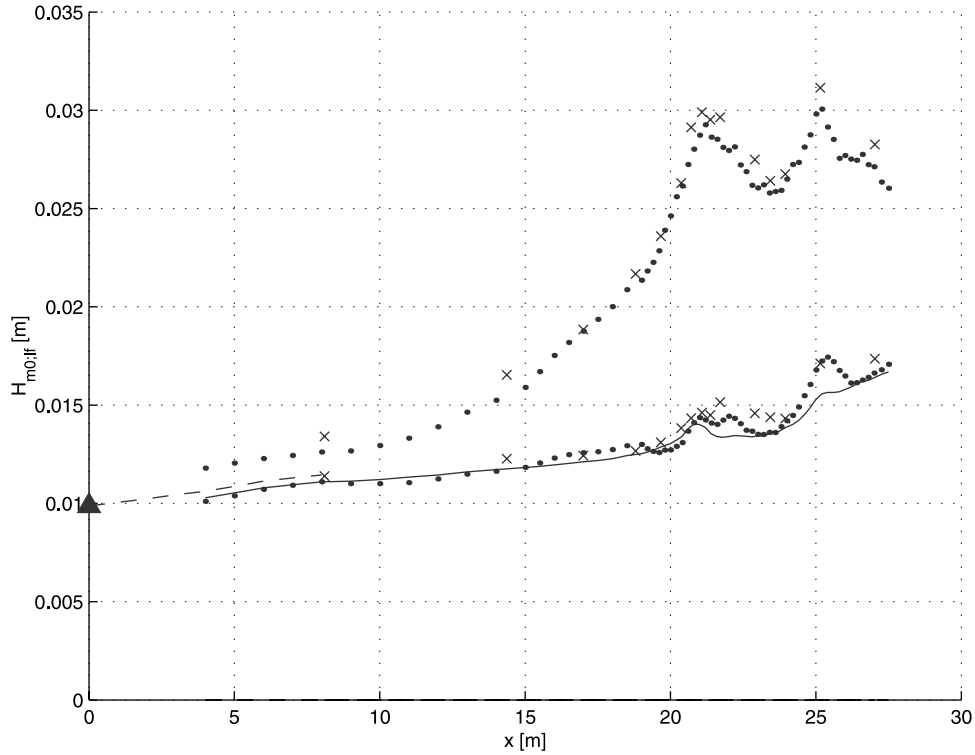

Figure 4. $H_{m_0,lf}$ values for incoming (upper set of data) and outgoing (lower set of data) lf waves, based on array method (dots) and colocated method (crosses). Dashed curve: Green's law over approach slope, initiated with LHS62 solution in the constant depth portion (dark triangle). Drawn curve: Green's law initiated with outgoing wave height at x = 8 m.

improvements in the calculated separation compared to a uniform wave approximation, particularly due to the inclusion of variation of the phase speed across the local array. Thus

$$Q^{\pm}_{m,p,r} = \left[c^{\pm}_{g,r}/c^{\pm}_{g,p}\right]^{1/2} e^{i\left(\psi^{\pm}_{m,p}-\psi^{\pm}_{m,r}\right)} \tag{6}$$

Herein, c_g^+ (incoming, group-bound waves) is set equal to the linear theory group velocity of the primary waves at the peak frequency, and c_g^- (outgoing waves) is set equal to $\sqrt{gh}$, appropriate for free long waves. These velocity values have also been used in the calculation of the phases $\psi^{\pm}$, by integration of the corresponding wave number from x_p to x_r.

[27] The system of equations (5) consists of P equations with two unknowns, $Z^+_{m,r}$ and $Z^-_{m,r}$. Thus when $P > 2$, the system is overdetermined, for which a least squares solution can be found. The system of equations (5) can be written as

$$\underbrace{\begin{bmatrix} Q^+_{m,1,r} & Q^-_{m,1,r} \\ Q^+_{m,2,r} & Q^-_{m,2,r} \\ \vdots & \vdots \\ Q^+_{m,P,r} & -Q^-_{m,P,r} \end{bmatrix}}_{B} \begin{bmatrix} Z^+_{m,r} \\ Z^-_{m,r} \end{bmatrix} = \begin{bmatrix} Z_{m,1} \\ Z_{m,2} \\ \vdots \\ Z_{m,P} \end{bmatrix} \tag{7}$$

If the phase difference across the local array is relatively small, the matrix B becomes ill conditioned. The decomposition method then becomes highly sensitive to noise in the measurements. This means that a minimum array length is required to obtain stable estimates, which minimum can be decreased for decreasing water depth and increasing frequency. On the other hand, the assumptions used in equation (6) will introduce larger errors in the separation results for longer arrays. Thus there are conflicting demands on the array length. The results shown below are based on five-gauge local arrays for the higher frequencies ($f >$ 0.11 Hz) and on nine-gauge arrays for the remaining, lower frequencies.

[28] As a check on the wave gauge separation results, we applied the approach utilizing data from colocated sensors for horizontal particle velocity and surface elevation, assuming these variables to be related as in long waves [*Guza et al.*, 1984]. The principal advantage of this method in our application is that it is not affected by spatial variations in the wave field, unlike the gauge array method. Also, singular behavior does not occur because the corresponding matrix has nonzero eigenvalues, independent of the frequency. For these reasons, the colocated method is a good basis for testing the array method, but because velocity data were available at far fewer points in the cross-shore profile than the surface elevation data (see Figure 1), it is not preferred a priori for the final analyses.

5.2. Results for Total lf Wave Heights

[29] Although the separation procedure was carried out in the frequency domain, we first present results integrated over the lf spectrum. Figure 4 shows the cross-shore variation of the total wave height $H_{m_0,lf}$ for the incoming

as well as for the outgoing lf waves, estimated from the corresponding Fourier amplitudes according to

$$H^{\pm}_{m_0,lf} = 4\sqrt{\sum_{f_{min}}^{f_{max}} 2\left|Z^{\pm}_m\right|^2} \qquad (8)$$

for f_{min} = 0.03 Hz and f_{max} = 0.20 Hz. Results of both separation techniques are shown; they are in good agreement. This was also the case for the frequency bands separately (not shown here), indicating that the results of both can be considered reliable. In the remainder of this paper only the results of the wave gauge array method will be used, because the spatial coverage available for this method is much larger than it is for the colocated method (see Figure 1).

[30] Unfortunately, no data are available in the constant depth portion between the wave maker and the toe of the slope. Instead, the hf signal at the toe of the approach slope (at x = 0 m) was used to determine the value of the incoming $H_{m_0,lf}$ according to the LHS62 equilibrium solution (1), by integration of the local radiation stress spectrum (obtained from the spectrum of the hf envelope squared, see equation (13)) over the frequency range from 0.03 Hz to 0.2 Hz. (The use of the equilibrium solution is justified because of the second-order wave board control and because we use it only in the constant depth region.) The result (dark triangle in Figure 4) is somewhat lower than the value that would be obtained by extrapolation of the values observed over the slope to the toe location. The mild amplitude increase over the steep approach slope is of the order of that given by Green (short, dashed curve) and far less than according to the LHS62 equilibrium solution, which would be a factor of about 4 from the toe at x = 0 m (h = 0.75 m) to $x \cong 8$ m ($h \cong$ 0.40 m). We return to this in the Discussion.

[31] From the start of the more or less plane, mild (1:70) slope near x = 8 m to the crest of the outer bar near x = 21 m, the lf wave height increases from about 1.3 cm to about 3.0 cm, an enhancement factor of about 2.5, considerably exceeding the energy-conserving value (Green) of about 1.2. The corresponding gain in shoreward lf energy flux on that interval is about 3.5% of the hf incident flux, corresponding to a reduction in incident short-wave heights of less than 2%.

[32] The incident hf waves in the present case were of low steepness (initial H_{m_0} about 0.6% of the deep-water wavelength at the peak frequency). Higher-steepness incident waves break further offshore, i.e., in relatively deeper water. This shortens the cross-shore extent of effective energy transfer to the forced waves, because the forcing is considerably reduced when the short waves start breaking, as a result of the overall decrease in short-wave amplitude as well as the reduction in groupiness (see Figure 4). Therefore it is expected that the incoming bound waves are enhanced less in the shoaling zone as the incident short waves are steeper, and that consequently the relative amount of incident hf energy transferred to the subharmonics is reduced with increasing incident wave steepness, becoming even less than the small fraction mentioned above. This would imply that in many cases the transfer of short-wave energy to lf motions has a negligible effect on the short-wave energy balance in the shoaling zone.

[33] Figure 4 shows that at the most shoreward location for which separated lf signals are available (x = 28 m), the outgoing lf wave height is nearly 0.65 times the incident value at that same location, implying an energy loss shoreward of this location of about 60% of the local incident flux. This is a remarkably high value, considering the short stretch in which it occurs (2 m in the flume, or about 1/4 of the local wavelength of the most energetic lf components, with $f \cong 0.05$ Hz). About 95% of the hf energy is dissipated offshore of this region [*Boers*, 1996], so the inshore interval concerned is indeed the extreme shallow-water fringe of the profile (compare also with Figure 1). Analyses of data obtained at the Duck field site by *Henderson et al.* [2000] have also shown a significant dissipation of lf energy in a narrow strip near the waterline, particularly for moderate wave conditions with negligible dissipation on the bar. In a follow-up paper, *Henderson and Bowen* [2002] show that the observed nearshore dissipation is not inconsistent with a (quadratic) bottom friction process, using a reasonable value of the dimensionless resistance coefficient, but contributions from enhanced turbulence due to wave breaking and swash processes may be expected to play a role as well. In a similar analysis of the Duck data, *Sheremet et al.* [2002]) have likewise reported significant lf energy dissipation in the surf zone, as do *Baldock et al.* [2000] on the basis of their laboratory data. However, both these papers do not mention possible dissipation mechanisms.

[34] It can be seen in Figure 4 that the outgoing lf waves deshoal in close agreement with Green's law (plotted in the figure, initialized at x = 8 m), in agreement with previous results showing that these are free, long waves that essentially conserve energy on the cross-shore interval considered. (As we shall see below, this energy conservation does not hold over small propagation distances of discrete Fourier components of the outgoing lf waves, which exchange energy with the incident wave groups in an oscillatory manner.)

[35] Figure 4 shows that the heights of the incident lf waves exceed those of the outgoing waves at all measurement locations. This is consistent with the fact that for these experiments the strongest cross correlation between the short-wave envelope and the incoming lf signal at the same offshore location occurs at near-zero time lag [*Janssen et al.*, 2003], in contrast with the well-known observation by *Tucker* [1950] (and many after him) that the incident short-wave envelope at some offshore location was more strongly (negatively) correlated with the outgoing waves than with the incoming waves, as inferred from the time lag of strongest correlation. Thus, for those observations the outgoing lf waves were dominant compared to the incoming lf waves. This requires that shoreward of the (offshore) point of observation, the incident lf waves are enhanced more strongly than the outgoing waves deshoal. However, in the present experiments dissipation in the nearshore zone appears strong enough to prevent the outgoing components from becoming dominant, but it cannot be excluded that this would change for locations farther offshore, beyond the range of Boers' measurements, such that in those locations the outgoing lf waves would be dominant.

5.3. Results for lf Wave Heights per Frequency Band

[36] Following the preceding analysis of the total incoming and outgoing lf energy, we now consider this in a frequency-resolved manner. Figure 5 shows lf wave height values calculated with equation (8) for a number of separate

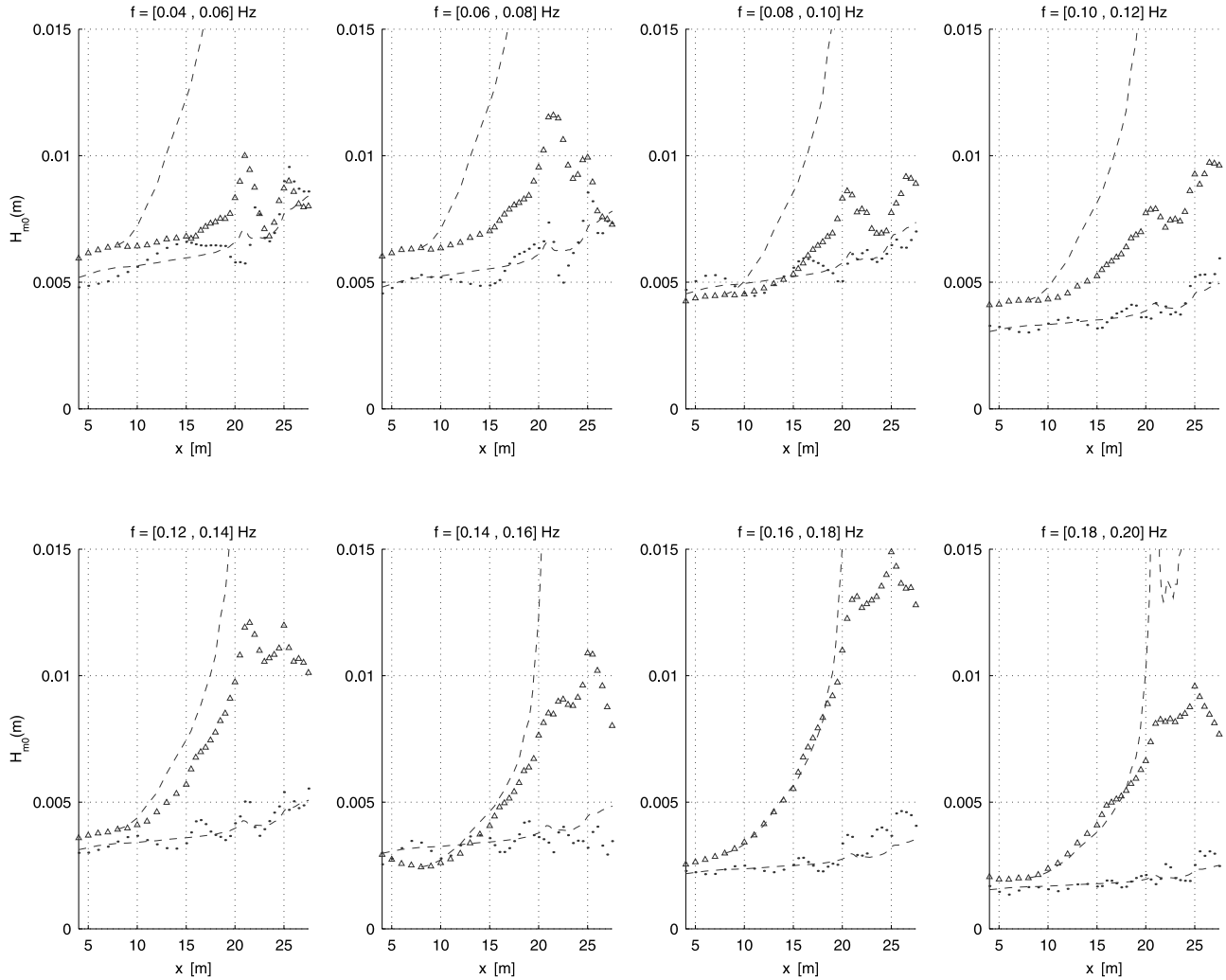

Figure 5. H_{m0} values of incoming (triangles) and outgoing (dots) lf waves for different frequency bands. Lower dashed curve: Green ($H \sim h^{-1/4}$), fitted to outgoing wave heights in the zone offshore from x = 20 m; upper dashed curve: LHS62 asymptote ($H \sim h^{-5/2}$), initiated with wave height at x = 8 m.

frequency bands with a width of 0.02 Hz. For comparison, the amplitude variation proportional to $h^{-5/2}$ is also shown, i.e., the shallow-water asymptote of the LHS62 equilibrium solution, initiated with the incoming lf wave height at the start of the gentle slope (x = 8 m), as well as a variation proportional to $h^{-1/4}$ as expected for free long waves (Green), fitted to optimally match the heights of the outgoing waves in the (de)shoaling zone.

[37] It can be seen in Figure 5 that the growth rate of the incoming lf waves increases significantly with frequency, being of the order of Green's law for the lower frequencies and comparable to the shallow-water limit of the LHS62 equilibrium solution for the highest of the (subharmonic) frequencies. The experimentally observed trend of increasing growth rate with increasing frequency is in agreement with field observations by *Elgar et al.* [1992] and with laboratory data presented by *Baldock et al.* [2000]. It confirms similar findings based on numerical integration of the forced long-wave equations [*van Dongeren*, 1997] or Boussinesq equations [*Madsen et al.*, 1997]. It implies a frequency-dependent effectiveness of the transfer of energy between hf and lf waves, to which we return below.

[38] In the above, we have referred to lf amplitude variations with depth (at high frequencies) comparable to the $h^{-5/2}$ variation of the near-resonant equilibrium solution for quasi-uniform forced waves over a sloping bed. Even where such amplitude-depth dependence exists, it does not necessarily imply that the equilibrium solution itself applies, because that prescribes an absolute value of the local lf amplitude in an algebraic dependence on the local depth and short-wave radiation stress with a given proportionality constant (equation (1)), in contrast with a shoaling law (such as Green) which leaves the proportionality constant in the solution undetermined. In the experiment analyzed here, the group-bound waves were enhanced very weakly over the steep approach slope, about a factor 4 less than predicted by the equilibrium solution. Therefore, even if the lf growth rate over the gentle slope would be proportional to $h^{-5/2}$, the local amplitudes there would fall short of their equilibrium values. This again underlines that the equilibrium solution of LHS62 is not a shoaling law.

[39] Returning to Figure 5, we see that shoreward of the offshore bar near x = 21 m the amplitude variation is no

longer monotonic, showing maxima due to enhanced depth-induced response near the crests of the offshore bar and an inner bar near $x = 25$ m. These variations are generally more pronounced for the incident waves and lower frequencies than for the outgoing waves and higher frequencies. The high growth rate of the higher-frequency components, apparent in the shoaling zone, is not continued shoreward of the outer bar. This is consistent with the release of the lf waves due to significant dissipation and/or saturation (loss of groupiness) of the primary waves in this region, although enhanced dissipation of lf wave energy due to the smaller depths and short-wave breaking may also play a role.

[40] At the most shoreward measurement location ($x = 28$ m), the heights of the outgoing and incoming lf waves are virtually the same for the lower frequencies, indicating almost full reflection at the shoreline (near $x = 30$ m). However, for higher frequencies the outgoing component is much weaker than the incoming component (about 1/3), implying a significant dissipation (about 90%) of the incoming lf energy in that frequency band in the narrow zone inshore of that location. Thus the lf dissipation commented on with reference to Figure 4 is not only localized in physical space but also in spectral space.

[41] An increase of dissipation of lf energy with increasing frequency is visible in the numerical results by *Schäffer and Jonsson* [1990] and *Roelvink* [1993], based on a model with quadratic bottom friction, and in the Duck field data as analyzed by *Henderson et al.* [2000]. It has been mentioned explicitly by *Madsen et al.* [1997], also based on numerical modeling. They hypothesize that this frequency dependence may in part be due to the numerical scheme being more dissipative for higher frequencies, but they also point to the fact that the higher-frequency subharmonics are less separated in frequency from the primary waves than the lower-frequency components, for which reason they could be more affected by dissipation due to the breaking of the primary waves. Observations by *Guza and Bowen* [1976] of suppression of subharmonic edge waves by breaking of higher-frequency primary waves have shown that such interaction is a realistic possibility. Since higher-frequency components are shorter than the lower-frequency components, their wavelength spans a smaller portion of the surf zone width (or may be only a fraction of it), for which reason they would be expected to suffer more dissipation from this. However, there is an indication that the dissipation noted in Boers' experiments may in fact be due to breaking of the subharmonic waves themselves, as explained in the Discussion (Section 7). The physical processes causing this inshore lf energy dissipation with a significant frequency dependence require further investigation.

[42] Last, we point out that the trends of the wave height variation of the outgoing lf components are in good agreement with Green's law, corresponding to energy-conserving long waves, independent of frequency, but more locally they show oscillations around this trend (Figure 5). These oscillations are due to interaction with the incoming short-wave groups, as we shall see in detail below.

6. Energy Transfer to lf Waves

[43] In this section we determine the energy transfer from the primary waves to the lf waves. This is done for the incoming and outgoing lf waves separately, using the energy balance equation (3) and the decomposition results from Section 5. To relate the local fluxes in these long waves to their local surface elevation, we use the quasi-uniform wave (WKB) approximation.

6.1. Incoming lf Waves

[44] The incoming forced waves are for the present purpose assumed to propagate with a phase speed equal to a representative group velocity c_g of the primary waves. For reasons of continuity, the volume flux, given by Uh, must equal $c_g\zeta$, from which it follows that $U = c_g\zeta/h$. The value of the (phase-averaged) energy flux in these forced waves is calculated on the basis of the long-wave velocity potential ϕ as

$$F = -\rho\left\langle \frac{\partial\phi}{\partial t}\frac{\partial\phi}{\partial x}\right\rangle h. \tag{9}$$

In view of the quasi-steady wave assumption, $\partial\phi/\partial t = -c_g\partial\phi/\partial x$, so that

$$F = \rho c_g\left\langle \left(\frac{\partial\phi}{\partial x}\right)^2\right\rangle h = \rho c_g\langle U^2\rangle h, \tag{10}$$

which for a specific spectral component with velocity amplitude $\hat{U}$ can be written as

$$F = \frac{1}{2}\rho\hat{U}^2 h c_g. \tag{11}$$

(This differs from the value for free long waves with a factor c_g^2/gh.) To approximate the phase-averaged rate of transfer of energy R defined in equation (3), we neglect the contribution of the gradient of the amplitude of the radiation stress compared to the contribution of the spatial phase variation (valid in the shoaling zone, which is the region on which we focus). The result can be written as

$$R \equiv -\left\langle U\frac{\mathrm{d}S_{xx}}{\mathrm{d}x}\right\rangle \cong \frac{1}{2}\kappa\hat{U}\hat{S}\sin(\Delta\psi), \tag{12}$$

in which $\kappa = 2\pi f/c_g$, the lf wave number, with c_g based on the peak frequency of the primary waves, and $\hat{U}$ and $\hat{S}$ denote the (real) amplitude of U and S_{xx} respectively, at the frequency considered.

[45] In order to estimate $\hat{S}$, the envelope of the observed short-wave signal at each gauge location ($A(t; x_p)$) has been determined using a low-pass-filtered Hilbert transform. Fourier coefficients of the squared hf envelope function (which is proportional to the local hf wave energy and radiation stress) have been determined as

$$V_{m,p} = \frac{1}{N}\sum_{j=1}^{N} A^2(x_p, t_j)e^{-i2\pi f_m t_j}. \tag{13}$$

These have been converted into radiation stress amplitudes using $S_{xx} = (2c_g/c - 1/2)E$.

[46] The phase lag ψ of the surface elevation of the incoming long waves behind the short-wave envelope at frequency f_m is determined from the observations through

$$\psi_{m,p} = \arg\left(V_{m,p}/Z^+_{m,p}\right). \tag{14}$$

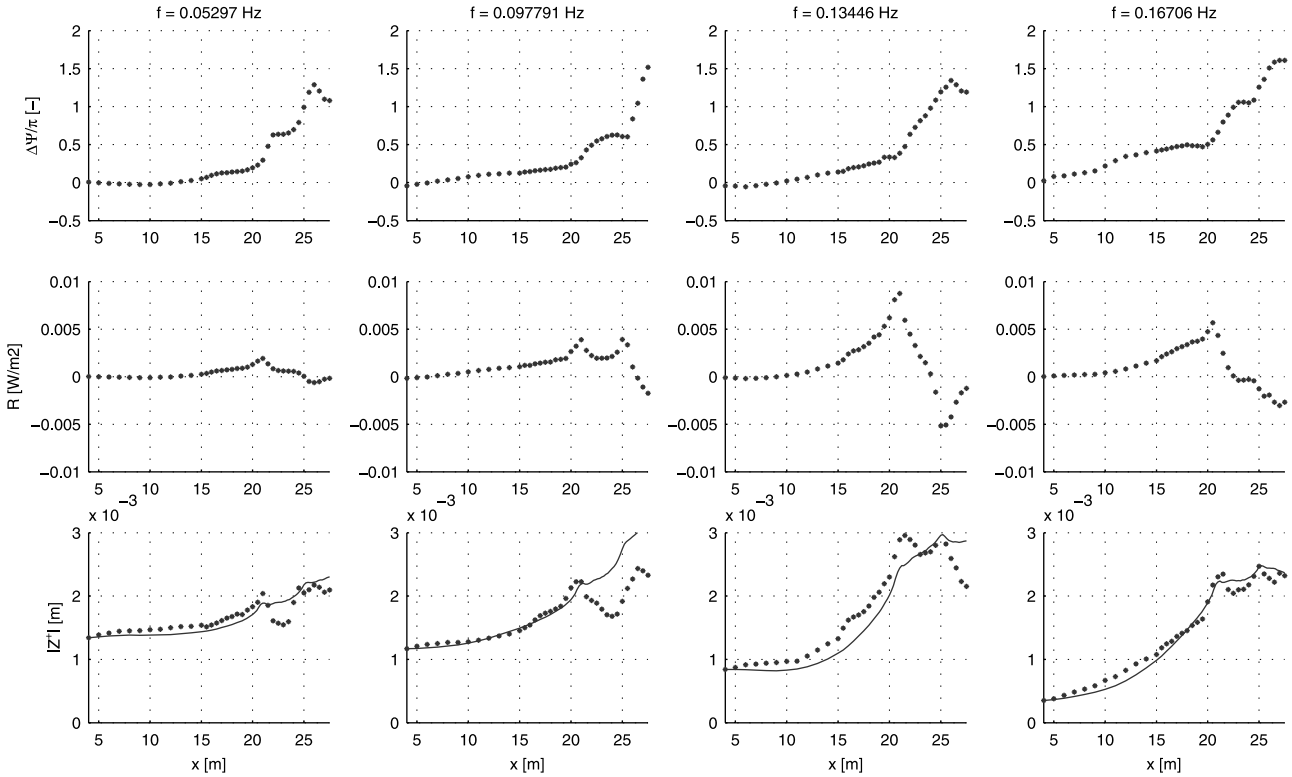

Figure 6. (top) Additional phase lag $\Delta\psi$ of incoming lf waves behind hf amplitude envelope. (middle) Corresponding source term R from equation (12). (bottom) Observed (dots) and computed (solid line) amplitudes of incoming lf waves.

The cross-shore variation of the additional lag $\Delta\psi \equiv \psi - \pi$ is given in Figure 6 (top), for four frequencies spanning the lf range. This shows that $\Delta\psi$ increases inshoreward direction, indicating that the incoming lf waves have a smaller propagation velocity than the hf envelope, as mentioned above (see *Janssen et al.* [2003] for a detailed analysis of the Boers data set in this respect). In the shoaling zone (offshore of the outer bar near $x = 21$ m), the phase lag $\Delta\psi$ varies more uniformly and more strongly for the higher frequencies than for the lower frequencies, for which the lag remains initially quite low. Interestingly, for all frequencies the lag reaches a value of approximately $\pi/2$ in the vicinity of the crest of the outer bar, i.e., in the region of initial breaking. This is reminiscent of similar behavior of bound superharmonics [*Elgar and Guza*, 1985]. The phase lag continues to increase inside the breaker region, reaching and exceeding values of π, in agreement with the positive zero lag correlation between hf envelope and lf surface elevation that has been reported numerous times for the surf zone.

[47] With the energy flux F given by equation (11) and the source term R given by equation (12), in which we substitute the values of $\hat{S}$ and $\Delta\psi$ obtained from the observations, the time-averaged lf energy balance (equation (3)) has for a sequence of distinct frequencies been integrated with respect to the cross-shore distance, taking the most offshore observed value as boundary value. (A similar analysis was carried out by *van Dongeren* [1997], using a numerical model exclusively, and by *van Dongeren et al.* [2002], with predicted values for $\hat{S}$ and $\Delta\psi$, the latter based on the theory by *Janssen et al.* [2003].) The resulting values of $\hat{U}$ have subsequently been converted into values of the surface elevation amplitude according to $\hat{\zeta} = \hat{U}h/c_g$. Figure 6 (middle) shows the values of the source function so obtained, and Figure 6 (bottom) shows the calculated and observed surface elevation amplitudes of the incoming lf waves.

[48] The agreement between calculated and observed values is fairly good to quite good in the shoaling zone. This confirms the validity of the applied model schematization, in particular the expression (12) for the work done on the lf waves by the grouped hf waves through the radiation stress and the neglect of dissipation (both restricted to the shoaling zone).

[49] The results show that the cross-shore variation of the energy transfer to the subharmonic waves (R) more or less mirrors the variation of sin $\Delta\psi$. This explains why, as mentioned above, the enhancement of the components with the lowest frequency is rather low, even near zero in the region $x < 15$ m, say, whereas those at higher frequencies are enhanced more strongly as a result of their larger phase lag over a greater distance in the shoaling zone. This difference can only be due to the different variations of the additional phase lag $\Delta\psi$, because the other factors in the right-hand side of equation (12) have comparable values in the entire shoaling zone for all frequencies.

[50] Calculated lf amplitudes inside the surf zone are also shown in Figure 6, but they are not expected to be reliable for various reasons. First, the radiation stress gradient dS_{xx}/dx was approximated in equation (12) by neglecting the contribution from the amplitude variation compared to that

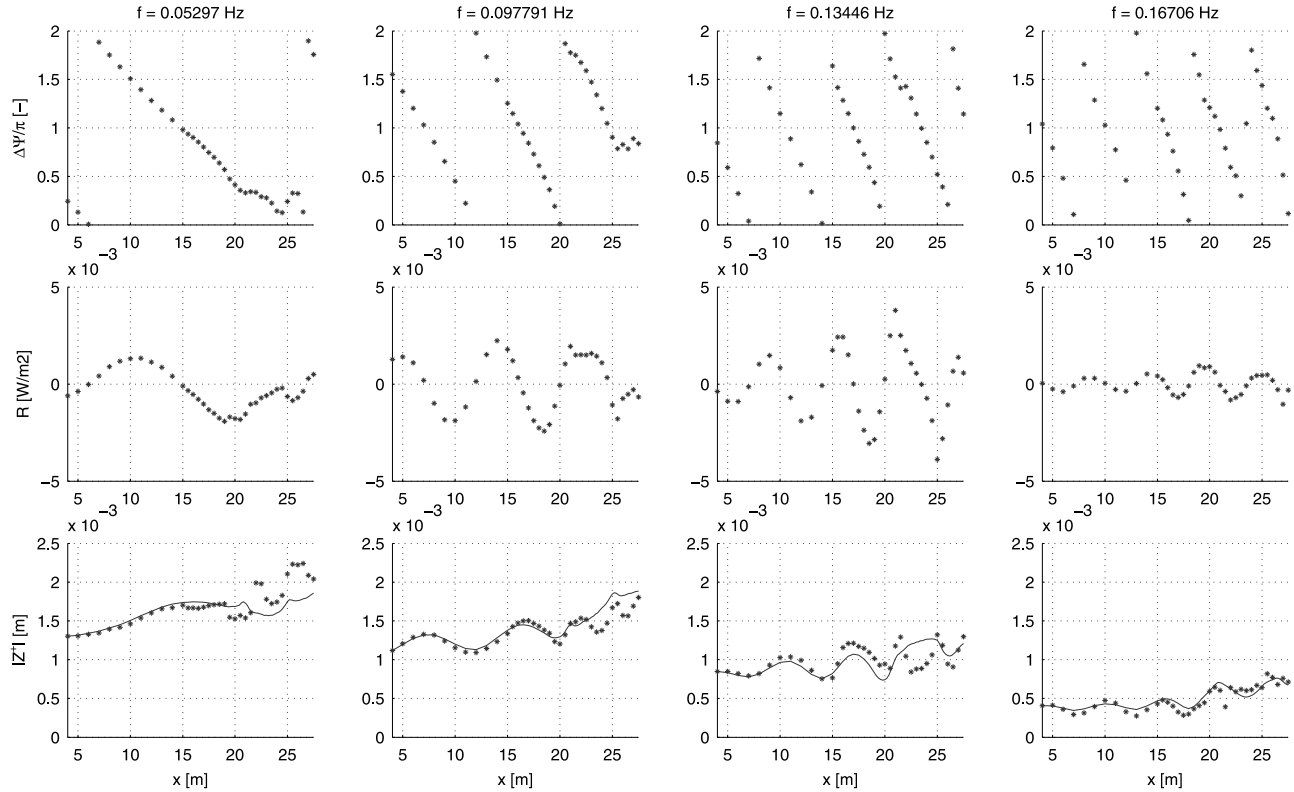

Figure 7. (top) Phase lag of outgoing lf waves behind hf amplitude envelope. (middle) Corresponding source term R from equation (12). (bottom) Observed (dots) and computed (solid line) amplitudes of outgoing lf waves.

from the phase variation. This should be a good approximation in the shoaling zone, but it cannot be expected to hold in regions of short-wave breaking; note that this also implies that the breakpoint generation mechanism is not modelled. Moreover, enhanced lf energy dissipation in the surf/swash zone will play a role, invalidating a priori the validity of equation (3). Finally, the use of small-amplitude theory for the translation of short-wave energy into radiation stress may not be accurate in the surf zone (although the results in the shoaling zone gave no indication for this, not even in the region just offshore of the outer bar where the short-wave breaking begins, and where such effects are usually maximal). For these reasons, the model for the energy transfer given above does not apply inside the breaker zone.

6.2. Outgoing lf Waves

[51] Numerical results by *van Dongeren* [1997] showed an oscillatory variation of the amplitude of outgoing periodic lf waves as a result of the repeated variation of the phase shift between these waves and the incident hf wave groups through cycles of 2π. These numerical results will now be subjected to empirical verification.

[52] The same calculation as for the incoming lf waves has been performed for the outgoing waves, except that the forced wave speed c_g has been replaced by the free wave speed $\sqrt{gh}$. The results are shown in Figure 7. Because the model for the energy transfer does not apply to the surf zone, the boundary condition for the integration of the energy balance of the outgoing lf waves has been located in the most offshore observation point.

[53] As noted above, an important difference with the incoming waves is that the phase difference between the incoming short-wave groups and the outgoing lf waves ($\Delta\psi$) varies rapidly through entire cycles from $-\pi$ to $+\pi$ because of the opposing directions of propagation (see Figure 7 (top)). This implies that energy is continually transferred back and forth between incident short-wave groups and outgoing long waves (Figure 7 (middle)), resulting in cross-shore oscillations in the lf amplitude (Figure 7 (bottom)) around a mean trend of amplitude decreasing in the propagation direction (offshore) because of deshoaling. Note that the transfer rate varies with x in phase with $\sin \Delta\psi$. In the shoaling zone, the computed amplitudes agree quite well with the observed values. The overall trend and the location and intensity of the oscillations are well reproduced. For the surf zone, the same comments apply as were made in the context of the incoming lf waves.

[54] The results shown in Figure 7 are for discrete frequencies. Across the spectrum, the oscillations in amplitude of the outgoing lf waves cancel out, resulting in a monotonic variation of total outgoing wave energy with depth due to energy-conserving deshoaling (Green's law, see Figure 4), although they are still clearly visible in the results for the 0.02 Hz frequency bands shown in Figure 5.

7. Discussion

[55] In this discussion we make an attempt at generalization of the results obtained, using a normalized bed slope as

an independent parameter. Following the definition of this parameter, we discuss its relevance to the dynamics of shoaling bound waves. This leads to a distinction between a so-called mild-slope regime and a so-called steep-slope regime. Next, we make some preliminary quantitative estimates of the characteristic values of the normalized bed slope bounding these regimes. We then consider its relevance for the relative importance of shoaled incident bound waves and breakpoint-generated waves. Finally, we consider the dependence of the nearshore dissipation of the incident subharmonic wave energy on the local normalized bed slope.

7.1. Normalized Bed Slope

[56] In the present experiment, the growth rate of shoaling forced lf waves has been found to increase with frequency, varying from weak enhancement for the lower frequencies (approximately $\sim h^{-1/4}$, Green's law) to the shallow-water limit of the equilibrium solution given by LHS62 ($\sim h^{-5/2}$) for the higher frequencies. This frequency dependence is for a specific set of values of other independent parameters that were not varied in the experiment, in particular the bed slope. Now it is well known that a given bed slope appears steeper, in a manner of speaking, to longer (lower-frequency) waves than it does to shorter (higher-frequency) waves, because the former experience a greater change in depth within a wavelength than the latter. This leads to a well-known dimensionless parameter, the normalized bed slope, expressing the relative depth change per wavelength. It can be written as $h_x/\kappa h$, in which h and h_x are characteristic values of depth and bed slope in the (sub)region considered and $\kappa = \omega/c_g$ is the wave number, where $\omega = 2\pi f$. Approximating c_g as $\sqrt{gh}$, we obtain the following dimensionless parameter (β) representing the normalized bed slope:

$$\beta \equiv \frac{h_x}{\omega}\sqrt{\frac{g}{h}} \tag{15}$$

The characteristic value of h to be used here depends on the region and the process considered; it will be specified in each particular case.

[57] A parameter that is closely related to β is the normalized surf zone width as defined for a plane slope by *Symonds et al.* [1982] in the context of their breakpoint generation model:

$$\chi \equiv \frac{\omega^2 h_b}{g h_x^2} \tag{16}$$

Here h_b is the depth at the mean breakpoint position. It follows that $\chi = \beta_b^{-2}$, in which the subscript b on β designates that we have substituted h_b for h. If in the expression for β we replace the depth by the incident wave height (indicated by the subscript H) the surf similarity parameter ξ [*Battjes*, 1974] or Iribarren number [*Iribarren and Nogales*, 1949] is obtained, except for a numerical constant: $\xi = \sqrt{2\pi}\beta_H$. We utilize this correspondence below.

[58] The relevance of the parameter β (or any of its equivalents) to the shoaling of forced group-induced long waves is supported by numerical calculations by *van Dongeren* [1997] and *Madsen et al.* [1997] using bichromatic primary waves. *Madsen et al.* [1997] found that the variations of calculated incoming lf amplitudes (at the most offshore breakpoint of the short waves) with the subharmonic frequency and the bed slope collapsed into a single-valued function of the ratio of frequency to bed slope, for fixed values of incident wave amplitude (this corresponds to a variation of β through variation of ω and h_x only). Applied to the present data set, this would imply that the observed increase of growth rate with frequency for a given slope can be translated into an expected decrease of growth rate with increasing slope for a given frequency. This is qualitatively in agreement with our observation that the lf shoaling over the much steeper approach slope was quite weak, in fact nearly like that of free waves, compared to the higher growth rate observed over the more gentle slope covering most of the shoaling zone. In other words, the data suggest a distinct difference between a steep-slope regime and a mild-slope regime, primarily controlled by the normalized bed slope. In the following we elaborate on this assumption and we make some tentative quantitative estimates of characteristic values differentiating between these regimes.

7.2. Quantitative Estimates

[59] Taking $h_x \cong 1{:}70$ and $h \cong 0.35$ m as representative values in the shoaling region in Boers' experiments (see Figure 1), and using $f = 0.04$ Hz and $f = 0.20$ Hz as transition frequencies for the transitions to weak enhancement and strong enhancement, respectively (see Figure 5), we find $\beta_s \cong 0.30$ and 0.06, respectively, where the subscript s refers to the shoaling zone. A value of β_s less than this lower limit is sufficiently small to allow an amplitude growth rate as in the equilibrium solution, as observed for the higher frequencies. (However, the corresponding phase lag deviates significantly from its equilibrium value. Indeed, as noted previously, that is a necessary condition for a growth proportional to $h^{-5/2}$ in view of the energy gain required for this.) On the contrary, a value of β_s exceeding the upper limit of about 0.3 appears to be sufficiently large for the free-wave solution to apply in reasonable approximation, as observed for the lower frequencies. These estimated transition values are tentative, because we have used only one data set in this estimation. Moreover, it is not clear in general which depth would be characteristic for the shoaling zone, thus making the appropriate value of β_s somewhat subjective. Future work may shed more light on this.

[60] Over the steep approach slope, frequency-resolved results are not available. Using a central frequency for the LF motions of about 0.1 Hz as representative for the overall LF motion, in combination with $h \cong 0.6$ m and $h_x \cong 1{:}20$, we find a β_s value of about 0.3, implying a steep-slope regime, in agreement with the observed weak enhancement of the total incoming lf wave height, which more or less follows Green's law (Figure 4).

[61] What can be said about the behavior to be expected in general? A given slope will always appear to be "steep", in the present meaning, to waves of sufficiently low frequency. Therefore the lower-frequency components of the subharmonic waves are expected to shoal in the steep-slope regime, approximately like free waves. In contrast, if the bandwidth of the incident hf waves is sufficient, energetic lf components may reach sufficiently high fre-

quencies for the mild-slope regime, implying an effective energy transfer from the grouped short waves and significant excess growth compared to shoaling of free waves. It would follow from this analysis that the rate of enhancement of the total lf energy in general is between that for free waves and the local equilibrium solution (this is what in fact has invariably been observed), depending on the spectrum (characteristic frequency and bandwidth) and the cross-shore bottom profile, so that no general relationships are expected to hold. Moreover, more parameters play a role, in particular the short-wave steepness. Higher steepness implies earlier breaking, which is expected to lead to smaller total enhancement of the forced waves. A more detailed analysis is required to draw firm conclusions in this direction.

7.3. Relative Importance of Shoaled Bound Waves and Breakpoint-Generated Waves

[62] Next, we consider the relative intensity of the shoaled bound lf waves and the lf waves generated by the moving breakpoint [*Symonds et al.*, 1982]. In the latter theory, the amplitudes of outgoing lf waves, for weakly modulated bichromatic incident hf waves on a plane slope, vary in an oscillatory manner with the parameter χ defined in equation (16), reaching a first maximum for $\chi \cong 1$, implying $\beta_b \cong 1$ since $\chi = \beta_b^{-2}$. Even when taking into account that h_b is smaller than the depth used for the shoaling zone, this is well in the "steep-slope" regime as defined above for the subharmonic waves, in which hardly any enhancement of the lf waves is expected other than free-wave shoaling, because of ineffective energy transfer to the long waves by the grouped short waves. So, in the steep-slope regime the breakpoint-generated waves are expected to dominate over the (weakly) enhanced incident forced waves. In contrast, the breakpoint generation is ineffective for $\chi \gtrsim 10$ because of phase cancellation, as argued by *Baldock and Huntley* [2002]. (The criterion which they give can be cast in the form given here.) This corresponds to $\beta_b \lesssim 0.3$, and to a smaller upper limit for β_s (because the depth in the shoaling zone is greater than at breaking), bringing us outside the steep-slope regime. Thus, in the mild-slope regime the breakpoint generation is ineffective whereas for those conditions the incident bound waves are enhanced strongly and may therefore be expected to dominate. These results lend support to and generalize the suggestion by *List* [1992] and the conclusion by *van Dongeren et al.* [2002] that the fraction of the total nearshore lf energy due to incident bound waves, relative to contributions from breakpoint-generated waves, increases with decreasing bed slope.

7.4. Nearshore Dissipation of Subharmonic Waves

[63] Finally, we consider the dissipation of lf energy near the waterline. The reflection/absorption of the lf waves in this region has been seen to be frequency dependent. It is well known that wind waves and swell incident on a slope may be almost fully reflected if they do not break on the slope, and be almost fully absorbed if they do. Here too we can refer to a (local) steep-slope regime and a mild-slope regime, in this case in the context of surf similarity [*Battjes*, 1974]. Both regimes are separated by a transition value $\xi \cong 2.5$, implying $\beta_H \cong 1$. We tentatively apply this transition criterion to the incoming lf waves shoreward of the limit of the data points shown in Figures 4 and 5, in the region near the waterline. The bottom there is virtually plane at a slope of about 1:25 (Figure 1). Combined with a value of 0.025 m for the incident lf wave height, as read from Figure 4, and a critical value $[\beta_{H_{lf}}]_{cr} \cong 1$, we obtain an estimated transition frequency of about 0.12 Hz. Inspection of Figure 5 shows that indeed this frequency is in the transition range between almost full reflection at lower frequencies and strong dissipation (≅90%) at higher frequencies. Even though the application of a periodic wave criterion to random waves has some numerical uncertainty, this result does suggest that the significant dissipation of the higher-frequency subharmonics in the narrow strip near the waterline, that was already commented on in Section 5.3, may be due to breaking of these waves. However, we have no direct other evidence to support this suggestion. For completeness' sake, we note that a breaking criterion as used here has previously been shown to be applicable to a very wide range of wave steepness and bottom slope, even including tsunamis and tides [*Munk and Wimbush*, 1969], so that applicability to these low-steepness, subharmonic waves cannot be ruled out a priori.

8. Conclusions

[64] A high-resolution laboratory data set of one-dimensional random wave propagation over a barred beach has been subjected to a detailed analysis. The results confirm and extend previous work.

[65] The previously reported phase lag of the shoaling incident forced waves behind the forcing short-wave groups is confirmed. Its key role in the growth of the shoaling forced waves due to energy transfer from the grouped short waves is highlighted and used to calculate the cross-shore variation of the rate of this transfer.

[66] The observed growth rate of the amplitudes of the incoming lf waves in the shoaling zone varies from nearly that of free long waves ($\sim h^{-1/4}$, Green's law) for the lower subharmonic frequencies to nearly the shallow-water limit of the equilibrium solution given by *Longuet-Higgins and Stewart* [1962] ($\sim h^{-5/2}$) for the higher lf frequencies. The enhancement of the forced incoming long waves in the shoaling zone is predicted quite accurately on the basis of the estimated rates of energy transfer from the hf waves to the lf waves. The normalized bed slope $h_x/\kappa h$, or $(h_x/\omega)\sqrt{g/h}$, appears to be an important or even controlling parameter in this respect. It is seen to differentiate between relatively mild slopes (relative to $\omega \sqrt{h/g}$), for which the enhanced incident bound waves are expected to dominate over contributions from breakpoint generation, and steep slopes in which the opposite is expected, but further inquiry is necessary for firm conclusions in this respect, in which also the characteristics of the primary waves should be considered.

[67] The accuracy of the lf amplitude prediction based on a dissipationless model in the shoaling zone is an indication of negligible lf energy dissipation there. The incident lower-frequency subharmonics are nearly fully reflected at the shoreline, but the higher-frequency lf components appear to be subject to a significant dissipation in a narrow inshore zone including the swash zone, totalling (in this experiment) about 90% of the local incident lf energy in that frequency

band and about 60% of the total local incident lf energy. There is an indication that this dissipation may be due to breaking of the higher-frequency subharmonic waves.

[68] The outgoing lf wave components exchange energy with the incoming short-wave groups in an oscillatory fashion, because of the rapidly varying phase difference between these wave systems that travel in opposite directions. Averaged across the spectrum and/or over larger distances, these effects cancel out and the amplitude varies as for free waves (Green's law).

Notation

A envelope of high-frequency incident waves, m.
c phase velocity of high-frequency incident waves, m/s.
c_g group velocity of high-frequency incident waves, m/s.
f frequency, Hz.
f_p peak frequency of high-frequency incident waves, Hz.
F time-averaged energy flux per unit span in low-frequency waves, W/m.
g gravitational acceleration, m/s^2.
h mean water depth, m.
h_b mean depth at mean breakpoint position, m.
H_{m_0} significant wave height (four times the standard deviation of the surface elevation in the frequency range considered), m.
k wave number of high-frequency incident waves, rad/m.
R rate of energy transfer per unit area from grouped short waves to forced long waves, W/m^2.
S_{xx} component of radiation stress of high-frequency incident waves, N/m.
$\hat{S}$ (real) amplitude of Fourier component of S_{xx}, N/m
t time, s.
U depth-averaged particle velocity in progressive long wave, m/s.
$\hat{U}$ (real) amplitude of Fourier component of U, m/s.
V (complex) Fourier component of A^2, m^2.
x cross-shore coordinate, positive onshore, m.
Z (complex) Fourier component of low-frequency surface elevation, m.
β normalized bed slope
ζ surface elevation of low-frequency motion, m.
κ wave number of low-frequency motion, rad/m.
ξ surf similarity parameter
ρ mass density, kg/m^3.
σ frequency of high-frequency incident waves, rad/s.
χ normalized surf zone width
ψ phase difference between short-wave envelope and bound wave, rad.
$\Delta\psi$ phase lag of bound wave behind equilibrium value, rad.
ω frequency of low-frequency motion, rad/s.

[69] **Acknowledgments.** This work was performed in the framework of the Dutch Center for Coastal Research with sponsoring by the National Institute for Coastal and Marine Management (HJB) and WL/Delft Hydraulics (ARvD). The authors thank Marien Boers for providing the original data of his precious experiments.

References

Agnon, Y., and A. Sheremet (1997), Stochastic nonlinear shoaling of directional spectra, *J. Fluid Mech.*, *345*, 79–99.

Baldock, T. E., and D. A. Huntley (2002), Long-wave forcing by the breaking of random gravity waves on a beach, *Proc. R. Soc. London, Ser. A*, *458*, 2177–2201.

Baldock, T. E., and D. J. Simmonds (1999), Separation of incident and reflected waves over sloping bathymetry, *Coastal Eng.*, *38*, 167–176.

Baldock, T. E., D. A. Huntley, P. A. D. Bird, T. O'Hare, and G. N. Bullock (2000), Breakpoint generated surfbeat induced by bichromatic wave groups, *Coastal Eng.*, *39*, 213–242.

Battjes, J. A. (1974), Surf similarity, in *Coastal Engineering 1974*, pp. 466–480, Am. Soc. of Civ. Eng., Reston, Va.

Biésel, F. (1952), *Équations Générales au Second Ordre de la Houle Irrégulière*, pp. 372–376, Houille Blanche, Paris.

Boers, M. (1996), Simulation of a surf zone with a barred beach, report 1: Wave heights and wave breaking, *Comm. Hydrol. Geotechnol. Eng. 96-5*, 116 pp., Delft Univ. of Technol., Delft, Netherlands.

Bowers, E. C. (1992), Low frequency waves in intermediate water depths, in *Coastal Engineering 1992: Proceedings of the Twenty-Third International Conference*, pp. 832–845, Am. Soc. of Civ. Eng., Reston, Va.

Chu, V. H., and C. C. Mei (1970), On slowly varying Stokes waves, *J. Fluid Mech.*, *41*, 873–887.

Eldeberky, Y., and P. A. Madsen (1999), Deterministic and stochastic evolution equations for fully dispersive and weakly non-linear waves, *Coastal Eng.*, *38*, 1–24.

Elgar, S., and R. T. Guza (1985), Observations of bispectra of shoaling waves, *J. Fluid Mech.*, *161*, 425–448.

Elgar, S., T. H. C. Herbers, M. Okihiro, J. Oltman-Shay, and R. T. Guza (1992), Observations of infragravity waves, *J. Geophys. Res.*, *97*, 15,573–15,577.

Foda, M. A., and C. C. Mei (1981), Nonlinear excitation of long-trapped waves by a group of short swells, *J. Fluid Mech.*, *111*, 319–345.

Freilich, M. H., and R. T. Guza (1984), Nonlinear effects on shoaling surface gravity waves, *Philos. Trans. R. Soc. London, Ser. A*, *311*, 1–41.

Guza, R. T., and A. J. Bowen (1976), Resonant interactions for waves breaking on a beach, in *Coastal Engineering 1976*, edited by B. L. Edge, pp. 560–579, Am Soc. of Civ. Eng., Reston, Va.

Guza, R. T., E. B. Thornton, and R. A. Holman (1984), Swash on steep and shallow beaches, in *Proceedings of the Coastal Engineering Conference, 1984*, edited by B. L. Edge, pp. 708–723, Am. Soc. of Civ. Eng., Reston, Va.

Hasselmann, K. (1962), On the non-linear energy transfer in a gravity-wave spectrum, *J. Fluid Mech.*, *49*, 481–500.

Henderson, S. M., and A. J. Bowen (2002), Observations of surf beat forcing and dissipation, *J. Geophys. Res.*, *107*(C11), 3193, doi:10.1029/2000JC000498.

Henderson, S. M., S. Elgar, and A. J. Bowen (2000), Observations of surf beat propagation and energetics, in *Coastal Engineering 1998: conference Proceedings*, edited by B. L. Edge, pp. 1412–1421, Am. Soc. of Civ. Eng., Reston, Va.

Herbers, T. H. C., and M. C. Burton (1997), Nonlinear shoaling of directionally spread waves on a beach, *J. Geophys. Res.*, *102*, 21,101–21,114.

Herbers, T. H. C., S. Elgar, and R. T. Guza (1994), Infragravity-frequency (0.005–0.05 Hz) motions on the shelf. part I: Forced waves, *J. Mar. Res.*, *24*, 917–927.

Iribarren, C. R., and C. Nogales (1949), Protection des Ports, paper presented at XVIIth International Navigation Congress, Permanent Int. Assoc. of Navig. Congr., Lisbon, Portugal.

Janssen, T. T., J. W. Kamphuis, A. R. Van Dongeren, and J. A. Battjes (2000), Observations of long waves on a uniform slope, in *Coastal Engineering 2000: Conference Proceedings*, edited by B. L. Edge, pp. 2192–2205, Am. Soc. of Civ. Eng., Reston, Va.

Janssen, T. T., J. A. Battjes, and A. R. Van Dongeren (2003), Long waves induced by short-wave groups over a sloping bottom, *J. Geophys. Res.*, *108*(C8), 3252, doi:10.1029/2002JC001515.

Kaihatu, J. M., and J. T. Kirby (1995), Nonlinear transformation of waves in finite water depth, *Phys. Fluids*, *7*, 1903–1914.

Kostense, J. K. (1984), Measurements of surf beat and setdown beneath wave groups, in *Proceedings of the Coastal Engineering Conference, 1984*, edited by B. L. Edge, pp. 724–740, Am. Soc. of Civ. Eng., Reston, Va.

List, J. H. (1992), A model for the generation of two-dimensional surfbeat, *J. Geophys. Res.*, *97*, 5623–5635.

Liu, P. L.-F. (1989), A note on long waves induced by short wave groups over a shelf, *J. Fluid Mech.*, *205*, 163–170.

Liu, P. L.-F., and M. W. Dingemans (1989), Derivation of the third-order evolution equations for weakly nonlinear water waves propagating over uneven bottoms, *Wave Motion*, *11*, 157–174.

Longuet-Higgins, M. S., and R. W. Stewart (1961), Changes in the form of short gravity waves on long waves and tidal currents, *J. Fluid Mech.*, *8*, 565–583.

Longuet-Higgins, M. S., and R. W. Stewart (1962), Radiation stress and mass transport in gravity waves, with application to 'surf beats', *J. Fluid Mech.*, *13*, 481–504.

Longuet-Higgins, M. S., and R. W. Stewart (1964), Radiation stresses in water waves: A physical discussion, with applications, *Deep Sea Res.*, *11*, 529–562.

Madsen, P. A., and O. R. Sørensen (1993), Bound waves and triad interactions in shallow water, *Ocean Eng.*, *15*, 371–388.

Madsen, P. A., O. R. Sørensen, and H. A. Schäffer (1997), Surf zone dynamics simulated by a Boussinesq type model. part II: Surf beat and swash oscillation for wave groups and irregular waves, *Coastal Eng.*, *32*, 289–319.

Mansard, E. P. D., and V. Barthel (1984), Shoaling properties of bounded long waves, in *Proceedings of the Coastal Engineering Conference, 1984*, edited by B. L. Edge, pp. 798–814, Am. Soc. of Civ. Eng., Reston, Va.

Masselink, G. (1995), Group bound long waves as a source of infragravity energy in the surf zone, *Cont. Shelf Res.*, *15*, 1525–1547.

Mei, C. C., and C. Benmoussa (1984), Long waves induced by short-wave groups over an uneven bottom, *J. Fluid Mech.*, *130*, 219–235.

Molin, B. (1982), On the generation of long-period second-order free-waves due to changes in the bottom profile, *Pap. Ship. Res. Inst. Tokyo*, *68*, 1–22.

Munk, W. H. (1949), Surf beats, *Eos Trans AGU*, *30*, 849–854.

Munk, W. H., and M. Wimbush (1969), A rule of thumb for wave breaking over sloping beaches, *Oceanology*, *9*, 56–59.

Phillips, O. M. (1977), *The Dynamics of the Upper Ocean*, 2nd ed., Cambridge Univ. Press, New York.

Reniers, A. J. H. M., A. R. Van Dongeren, J. A. Battjes, and E. B. Thornton (2002), Linear modelling of infragravity waves during Delilah, *J. Geophys. Res.*, *107*(C10), 3137, doi:10.1029/2001JC001083.

Roelvink, J. A. (1993), Surf beat and its effect on cross-shore profiles, Ph. D. diss., Delft Univ. of Technol., Delft, Netherlands.

Roelvink, J. A., H. A. H. Petit, and J. K. Kostense (1992), Verification of a one-dimensional surfbeat model against laboratory data, in *Coastal Engineering 1992: Proceedings of the Twenty-Third INternational Conference*, edited by B. L. Edge, pp. 960–973, Am. Soc. of Civ. Eng., Reston, Va.

Ruessink, B. G. (1998a), The temporal and spatial variability of infragravity energy in a barred nearshore zone, *Cont. Shelf Res.*, *18*, 585–605.

Ruessink, B. G. (1998b), Bound and free infragravity waves in the nearshore zone under breaking and nonbreaking conditions, *J. Geophys. Res.*, *103*, 12,795–12,805.

Schäffer, H. (1993), Infragravity waves induced by short wave groups, *J. Fluid Mech.*, *247*, 551–588.

Schäffer, H. A., and I. G. Jonsson (1990), Theory versus experiments in two-dimensional surf beats, in *Coastal Engineering Conference, 1990: Proceedings of the International Conference*, edited by B. L. Edge, pp. 1131–1143, Am. Soc. of Civ. Eng., Reston, Va.

Schäffer, H. A., and I. A. Svendsen (1988), Surf beat generation on a mild slope, in *Coastal Engineering, 1988*, pp. 1058–1072, Am. Soc. of Civ. Eng., Reston, Va.

Sheremet, A., R. T. Guza, S. Elgar, and T. H. C. Herbers (2002), Observations of nearshore infragravity waves: Seaward and shoreward propagating components, *J. Geophys. Res.*, *107*(C8), 3095, doi:10.1029/2001JC000970.

Symonds, G., and A. J. Bowen (1984), Interactions of nearshore bars with incoming wave groups, *J. Geophys. Res.*, *89*, 1953–1959.

Symonds, G., D. A. Huntley, and A. J. Bowen (1982), Two dimensional surfbeat: Long wave generation by a time varying breakpoint, *J. Geophys. Res.*, *87*, 492–498.

Tucker, M. J. (1950), Surf beats: Sea waves of 1 to 5 min. period, *Proc. R. Soc. London, Ser. A*, *202*, 565–573.

van Dongeren, A. R. (1997), Numerical modeling of quasi-3d nearshore hydrodynamics, *Res. Rep. CACR-97-04*, 243 pp., Cent. for Appl. Coastal Res., Univ. of Delaware, Newark.

van Dongeren, A. R., H. J. Bakkenes, and T. T. Janssen (2002), Generation of long waves by short wave groups, in *Coastal Engineering 2002*, edited by J. Smith McKee, World Sci., River Edge, N. J.

van Dongeren, A. R., A. J. H. M. Reniers, J. A. Battjes, and I. A. Svendsen (2003), Numerical modeling of infragravity wave response during Delilah, *J. Geophys. Res.*, *108*(C9), 3288, doi:10.1029/2002JC001332.

Van Leeuwen, P. J. (1992), Low frequency wave generation due to breaking waves, Ph. D. diss., Delft Univ. of Technol., Delft, Netherlands.

Van Leeuwen, P. J., and J. A. Battjes (1990), A model for surfbeat, in *Coastal Engineering Conference, 1990: Proceedings fo the International Conference*, edited by B. L. Edge, pp. 151–164, Am. Soc. of Civ. Eng., Reston, Va.

Van Leeuwen, P. J., and G. Klopman (1996), A new method for the generation of second order random waves, *Ocean Eng.*, *23*, 167–192.

Zelt, J. A., and J. E. Skjelbreia (1992), Estimating incident and reflected wave fields using an arbitrary number of wave gauges, in *Coastal Engineering 1992: Proceedings of the Twenty-Third International Conference*, edited by B. L. Edge, pp. 777–789, Am. Soc. of Civ. Eng., Reston, Va.

H. J. Bakkenes, Heerema Marine Contractors, Vondellaan 47, 2332 AA Leiden, Netherlands.

J. A. Battjes and T. T. Janssen, Section of Environmental Fluid Mechanics, Faculty of Civil Engineering and Geosciences, University of Technology, P. O. Box 5048, 2600 GA Delft, Netherlands. (j.battjes@ct.tudelft.nl)

A. R. van Dongeren, WL/Delft Hydraulics, P.O. Box 177, 2600 MH Delft, Netherlands.